

# On the driven Frenkel-Kontorova model: II. Chaotic sliding and nonequilibrium melting and freezing

Torsten Strunz and Franz-Josef Elmer

*Institut für Physik, Universität Basel, CH-4056 Basel, Switzerland*

(submitted to Phys. Rev. E, September, 1997, revised Jan. 98)

The dynamical behavior of a weakly damped harmonic chain in a spatially periodic potential (Frenkel-Kontorova model) under the subject of an external force is investigated. We show that the chain can be in a spatio-temporally chaotic state called fluid-sliding state. This is proven by calculating correlation functions and Lyapunov spectra. An effective temperature is attributed to the fluid-sliding state. Even though the velocity fluctuations are Gaussian distributed, the fluid-sliding state is clearly not in equilibrium because the equipartition theorem is violated. We also study the transition between frozen states (stationary solutions) and molten states (fluid-sliding states). The transition is similar to a first-order phase transition, and it shows hysteresis. The depinning-pinning transition (freezing) is a nucleation process. The frozen state contains usually two domains of different particle densities. The pinning-depinning transition (melting) is caused by saddle-node bifurcations of the stationary states. It depends on the history. Melting is accompanied by precursors, called micro-slips, which reconfigure the chain locally. Even though we investigate the dynamics at zero temperature, the behavior of the Frenkel-Kontorova model is qualitatively similar to the behavior of similar models at nonzero temperature.

PACS numbers: 46.10.+z, 46.30.Pa, 68.35.Rh

## I. INTRODUCTION

Systems with many degrees of freedom which are pinned in some external potential are very common in condensed matter. Examples are fluid-fluid interfaces in porous media [1,2], flux-lattices in type-II superconductors [3], and charge density waves [4] to mention only a few. Also dry friction (i.e., solid-solid friction) belongs to this class of systems because the asperities of the surfaces interlock.

A common feature of all these systems is a strongly nonlinear mobility. If one applies some field or force  $F$  on the system, the mobility is zero below some usually well-defined threshold  $F_c$ . Above this threshold the mobility is nonzero. In general it is some nonlinear function of the applied force  $F$ . The transition from a pinned system with zero mobility to a depinned one with some finite, nonzero mobility is called the *pinning-depinning transition*. It can be understood as a kind of “melting” which happens far from thermal equilibrium. The process is a typical nonequilibrium one because of two reasons. First, there is no ground state for  $F \neq 0$  and the pinned system has to be in some metastable state. Due to thermal fluctuations the system can overcome the barrier of the metastable state and move into another metastable state with less energy. This phenomenon leads to *creeping*

with a very low mobility. Second, beyond the pinning-depinning transition energy flows through the system at a constant rate which is given by the mobility times  $F^2$ . This flow is usually not small. Thus it cannot be deduced from linear response theory which works only near thermal equilibrium. The mobility of the sliding state strongly depends on the kind of energy dissipation.

The inverse process of this nonequilibrium melting is the *depinning-pinning transition* which is a kind of nonequilibrium “freezing”. Both kind of transitions do not have to occur at the same value of the applied force  $F$ . The behavior depends strongly on whether the degrees of freedom (i.e., flux lines, atoms etc.) have inertia or inertia is negligible compared to dissipative forces. In the case of strong dissipation the motion is overdamped. The pinning-depinning transition is in most cases of second order and indistinguishable from the depinning-pinning transition. Typical examples for such systems are flux lines in type-II superconductors and charge-density waves. If the motion is underdamped, hysteresis is possible because the inertia can overcome a pinning center. This is intuitively clear if one imagines the simplest model system of this kind, namely a particle in a spatially periodic potential [5].

Another important aspect of the collective behavior of pinned systems is whether the potential caused by the pinning centers is regular or irregular (quenched randomness). Often the pinning landscape is random. This case together with a purely dissipative diffusion-like dynamics has been studied extensively in the literature [6,7].

The aim of this paper is to study the opposite case in a fairly simple model, namely, the Frenkel-Kontorova (FK) model [8]. There is no quenched randomness. All pinning centers are identical forming a regular array. Furthermore, all pinned objects are identical and have a mass. The damping is assumed to be weak. We will see that weak damping is responsible for randomness that is caused by chaotic motion. Important physical applications of the FK model are arrays of identical Josephson junctions [9] and adsorbate layers on clean crystal surfaces [10].

In this paper we consider the one-dimensional FK model. The equation of motion (in dimensionless units) reads

$$\ddot{x}_j + \gamma \dot{x}_j = x_{j-1} + x_{j+1} - 2x_j - b \sin x_j + F, \quad (1)$$

where  $x_j$  is the position of particle  $j$ ,  $\gamma$  is the damping constant,  $b$  is the strength of the external potential, and  $F$  is the external force. The time derivative is denoted by a dot. In order to avoid effects due to the boundary layers we choose periodic boundary conditions, i.e.,

$$x_{j+N} = x_j + 2\pi M, \quad (2)$$

where  $N$  is the number of particles and  $M$  is an arbitrary integer. The periodic boundary conditions fixes the average particle distance  $a$  to  $a = 2\pi M/N$ . Because of symmetry  $a$  can be restricted to interval  $[0, \pi]$  without loss of generality.

Together with the previous paper [11] in which we have already investigated periodic and quasiperiodic solutions, the aim is to give a detailed investigation of the dynamical behavior in the weakly damped case for long chains (i.e.,  $N > 100$ ).

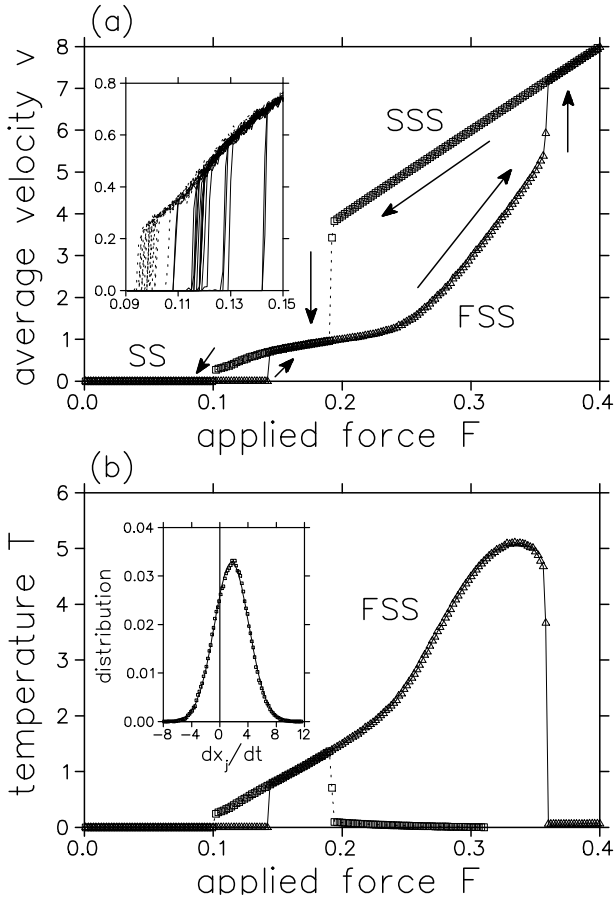


FIG. 1. The velocity-force characteristic and the effective temperature of the fluid-sliding state. The different branches belong to stationary states (SS), fluid-sliding states (FSS), and solid-sliding states (SSS). In the simulations the applied force  $F$  was decreased (squares and dotted lines) or increased (triangles and solid lines) with a constant rate ( $|\dot{F}| = 10^{-7}$ ). The velocity at each data point is the average over a time interval of  $10^4$  time units. The upper inset shows 20 hysteresis loops between SS and FSS from a simulation where  $F$  was moved in the interval  $[0.09, 0.15]$  forward and backward at a rate of  $|\dot{F}| = 10^{-6}$ . The lower inset shows the particle velocity distribution for  $F = 0.26$ . The solid line shows the fit of the data point with a Gaussian. The parameters are  $N = 233$ ,  $M = 89$ ,  $b = 2$ , and  $\gamma = 0.05$ .

In this paper we deal with spatio-temporal chaotic solutions (called *fluid-sliding states*) and the transition between these solutions and the stationary states. The typical behavior is summarized in figure 1. Fig. 1(a) shows the velocity-force characteristic. We see hysteresis loops between three different branches which belong to differ-

ent types of solutions. The states with the largest average sliding velocities  $v$  are the *solid-sliding states* which are characterized by a chain with nearly no internal vibrations. These states have the maximum possible mobility, i.e.,  $1/\gamma$ . The solid-sliding state becomes unstable due to first-order parametric resonance if  $v$  is below some critical value [11].

The second type of sliding state is the fluid-sliding state. In general one can summarize all sliding states having not the maximum mobility into this category. But strictly speaking the name makes only sense if these states are spatio-temporally chaotic. For larger values of the damping constant this is not the case as we have seen in the previous paper. The chaotic vibration in the fluid-sliding state can be characterized by an *effective temperature*. The temperature of the fluid-sliding states of Fig. 1(a) is shown in figure 1(b). Even though the distribution of the particle velocity  $\dot{x}_j$  is gaussian [see inset of Fig. 1(b)] we will show that the fluid-sliding state is a *nonequilibrium* state. A very specific test to show this is the violation of the equipartition theorem for the phonon modes (see Sec. II A).

The third type of states are the stationary ones. Their mobility is zero. In order to model the creeping due to thermal activation one has to add a white-noise term to the equation of motion (1). We have not done this because the qualitative behavior does not change very much as long as the thermal energy is much smaller than the amplitude of the external potential. This is confirmed in numerical simulations of similar models [10,12,13]. For example, the hysteresis seen in Fig. 1(a) still exist for nonzero but small temperatures [10,14]. For this behavior it seems to be important that the system has many degrees of freedom because in the case of  $N = 1$  the hysteresis disappears even for infinitesimal small noise amplitude [5].

Fig. 1(b) clearly shows that nonequilibrium melting and freezing is accompanied by an abrupt change of the temperature of the chain. The transition is like a first-order one in thermal equilibrium but the pinning-depinning transition point is larger than the depinning-pinning transition point. Thus hysteresis occurs. The transition points fluctuate [see inset of Fig. 1(a)], especially the pinning-depinning transition point.

The paper is organized as follows: In section II we investigate in detail the fluid-sliding state. We show that it is indeed spatio-temporally chaotic. For chains with  $a/2\pi$  near an integer value we found a pronounced transition from a kink-dominated sliding state and the fluid-sliding state. This transition is relatively sharp even though there is no hysteresis. But it becomes hysteretic for small  $N$ . The depinning-pinning transition and the pinning-depinning transition are discussed in section III. We show that nonequilibrium freezing is similar to ordinary freezing whereas melting is clearly different. The pinning-depinning transition point depends on the stationary state. Furthermore local rearrangements (micro-slips) of the chain may occur before the transition. In section IV we compare our results with results of similar models.

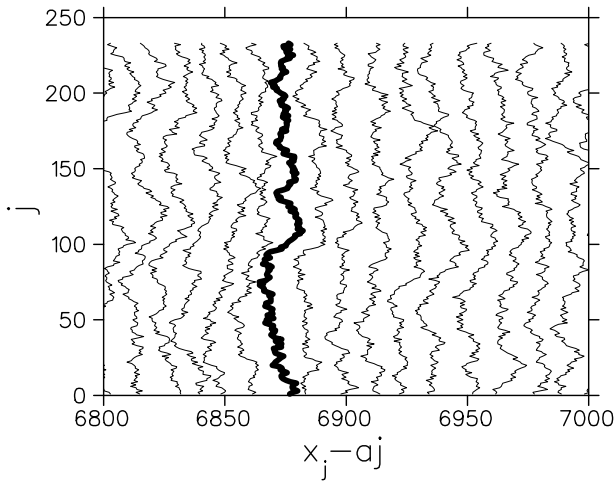


FIG. 2. An example for spatio-temporal chaos. Each solid line is a snapshot of the system. The time interval between two successive snapshots is  $\delta t = 4\pi/v$  ( $v$  is the average sliding velocity). A particular snapshot is highlighted. The parameters are  $N = 233$ ,  $M = 89$ ,  $b = 2$ ,  $\gamma = 0.05$ , and  $F = 0.14$ .

## II. CHAOTIC SLIDING

Decreasing the damping constant  $\gamma$  increases the complexity of the sliding state from periodic motion via quasi-periodic motion (which is usually spatially chaotic, see the preceding paper) to spatio-temporal chaos. An example of the latter one is shown in figure 2.

The aim of this section is to investigate and to characterize the chaotic-sliding state which we call the *fluid-sliding state*. First of all we see in Fig. 1(a) that the velocity-force characteristic of this state is nearly structureless. This has to be compared with the case of periodic and quasiperiodic motion where a multitude of hysteresis loops appear (see the preceding paper). Here there occur only hysteresis loops between the solid-sliding state (where the particles are shaken so fast that they nearly do not feel the external potential), the fluid-sliding state and the stationary states.

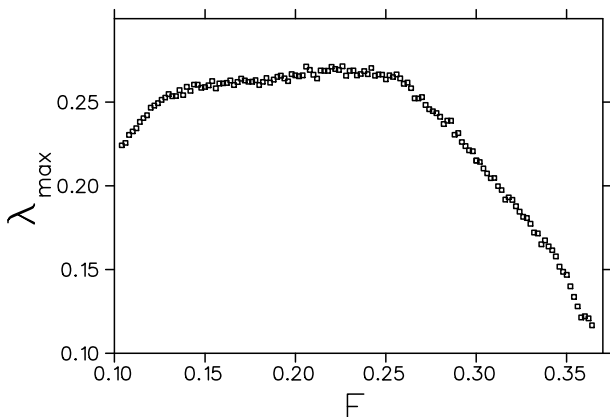


FIG. 3. The maximum Lyapunov exponent of the fluid-sliding state as a function of the applied force  $F$ . The parameters are  $N = 144$ ,  $M = 55$ ,  $b = 2$ , and  $\gamma = 0.05$ .

## A. Spatio-temporal chaos

Fig 2 is of course not a proof that the chain slides chaotically. It is well-known that chaotic motion is characterized by the sensitivity on the initial conditions. It is measured by the largest Lyapunov exponent  $\lambda_{\max}$ , which is the rate of divergence (or convergence, if it is negative) of trajectories in phase space that start out infinitely close to each other [15]. Figure 3 shows that the fluid-sliding states in Figs. 2 and 1 are indeed temporally chaotic.

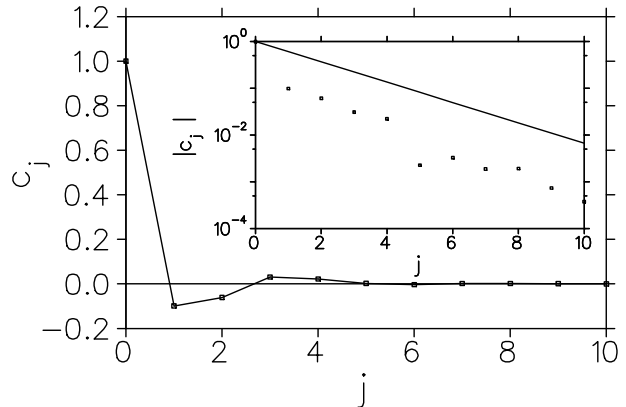


FIG. 4. The normalized velocity correlation function  $c_j$  of the fluid-sliding state. To guide the eye the numerical results (denoted by squares) are connected by a solid line. The inset shows a logarithmic plot of  $|c_j|$ . The straight line is the function  $\exp(-j/2)$ . The parameters are the same as in Fig. 2.

But is it also spatially chaotic? In order to answer this question we have calculated the normalized velocity correlation function  $C_j$  defined by

$$C_j \equiv \frac{\langle\langle \dot{x}_l \dot{x}_{l+j} \rangle\rangle - \langle\langle \dot{x}_l \rangle\rangle^2}{\langle\langle \dot{x}_l^2 \rangle\rangle - \langle\langle \dot{x}_l \rangle\rangle^2}, \quad (3)$$

where

$$\langle\langle f_j \rangle\rangle = \lim_{\tau \rightarrow \infty} \frac{1}{\tau} \int_0^\tau \frac{1}{N} \sum_{j=1}^N f_j(t) dt. \quad (4)$$

For the same parameters as in Fig. 2 the result is shown in figure 4. One clearly sees that  $C_j$  is a rapidly decaying oscillatory function. The envelope seems to be proportional to  $\exp(-j/\xi)$  with a correlation length  $\xi \approx 2$ . Because of  $N \gg \xi$  and  $\lambda_{\max} > 0$  the fluid-sliding state is spatio-temporally chaotic.

A very strong criterion for spatio-temporal chaos is that the number of positive Lyapunov exponents is proportional to  $N$  for large  $N$ . We have calculated the Lyapunov spectrum with the method described in Ref. [16] for various values of  $N$ . Figure 5 shows the cumulative density  $p_N(\lambda)$  of Lyapunov exponents, i.e., the probability to find a Lyapunov exponent larger than  $\lambda$ . The result is typical for spatio-temporal chaos [15]. In the thermodynamic limit (i.e.,  $N \rightarrow \infty$ ) the sequence of cumulative densities  $p_N$  converges uniformly to  $p_\infty$ . Thus, for large  $N$  the number of positive Lyapunov exponents is indeed

proportional to  $N$ . Fig. 5 shows clearly that the spatio-temporally chaotic nature of the fluid-sliding state does *not* depend on the commensurability of the chain.

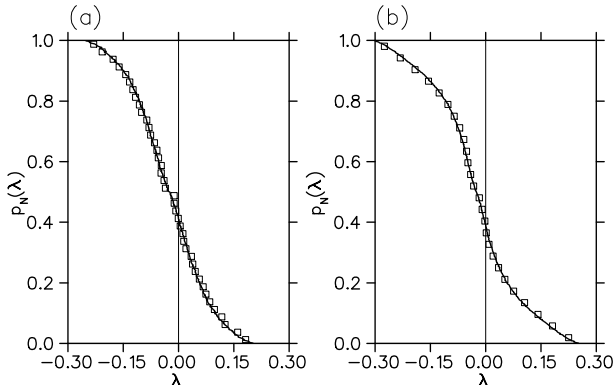


FIG. 5. Lyapunov spectra for (a) the most commensurate case (i.e.  $a = 0$ ) and (b) the most incommensurate case (i.e.  $a/2\pi \rightarrow (3 - \sqrt{5})/2 = 2 -$  golden mean). The spectra for two different system sizes are shown. Squares and solid lines denote (a)  $N = 20$ , (b)  $N = 13$ , and (a)  $N = 200$ , (b)  $N = 233$ . The other parameters are  $b = 2$ ,  $\gamma = 0.05$ , and (a)  $F = 0.13$ , (b)  $F = 0.3$ .

Because the fluid-sliding state is spatio-temporally chaotic it makes sense to introduce an effective *temperature*. In the dimensionless units of the equation of motion (1) it is the average kinetic energy in the frame co-moving with the center of mass, i.e.,

$$T \equiv \left\langle \left\langle \frac{(\dot{x}_j - v)^2}{2} \right\rangle \right\rangle, \quad (5)$$

where  $v$  is the average sliding velocity

$$v = \langle \dot{x}_j \rangle. \quad (6)$$

In the previous paper we have derived a formula for the applied force  $F$  in terms of the first and second moments of the particle velocity [Eq. (6) in Ref. [11]]. With the help of this formula the temperature can be expressed in terms of the applied force and the average sliding velocity:

$$T = \left( \frac{F}{\gamma} - v \right) \frac{v}{2}. \quad (7)$$

Figure 1(b) shows the temperatures of the fluid-sliding states of the velocity-force characteristic in Fig. 1(a).

Even though the temperature of the solid-sliding states and the stationary states is formally zero in accordance with (7), it does not make sense to call (5) a “temperature” in regular, non-chaotic sliding states or stationary states. The periodic and quasi-periodic domain-like states, for example, investigated in the previous paper have also non-zero “temperature”.

In the frame co-moving with the center of mass, the chain is shaken by the washboard wave (i.e., the external potential) and moves in a spatio-temporally chaotic way. The gaussian distributed velocities might suggest that the chain is in thermal equilibrium. But is it true? This raises the following question of general interest: *Can we*

*replace the spatio-temporally chaotic chain by an equivalent system which is in thermal equilibrium?* Or more general, is it possible to describe the chaotic attractor of a weakly damped and strongly driven Hamiltonian system with many degrees of freedom (infinitely many in the thermodynamic limit) by an equivalent undriven and undamped system? As a consequence of a positive answer one would expect that the equipartition theorem from thermodynamics holds, i.e. the ensemble averages of  $q_j \partial H / \partial q_j$  and  $p_j \partial H / \partial p_j$  are independent of  $j$  [ $H(q_1, p_1, \dots, q_j, p_j, \dots)$  is the Hamilton function, the  $q_j$ 's are the generalized coordinates, and the  $p_j$ 's are the corresponding canonical momenta]. In numerical simulations one usually replaces the ensemble average by the temporal average assuming that the ergodicity hypothesis holds. An obvious candidate for a test of the equipartition theorem would be the particle momentum in the co-moving frame, i.e.,  $\dot{x}_j - v$ . But this is not a wise choice: because of symmetry the result has to independent of  $j$ . A better choice is its spatial Fourier transform, i.e.,

$$\hat{p}_k \equiv \frac{1}{N} \sum_{j=1}^N (\dot{x}_j - v) e^{2i\pi k j / N}, \quad k = 0, 1, \dots, N - 1. \quad (8)$$

That is, we want to check whether the average kinetic energy

$$e_k \equiv \lim_{\tau \rightarrow \infty} \frac{1}{\tau} \int_0^\tau |\hat{p}_k(t)|^2 dt \quad (9)$$

of the phonon modes is equipartitioned or not. Figure 6 shows that the equipartition theorem is not fulfilled [17]. This is a clear signature for the fact that the *fluid-sliding state is a state far away from thermal equilibrium*. Therefore it is not possible to develop a theory for this state based on equilibrium thermodynamic. The violation of the equipartition theorem is equivalent with non-zero velocity correlations for  $j \neq 0$  because  $e_k$  is the modulus of the Fourier transform of  $C_j$ .

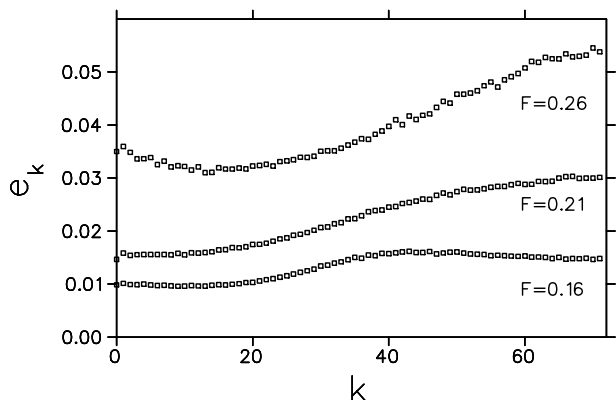


FIG. 6. The average kinetic energy  $e_k$  of the phonon modes for three different values of the applied force  $F$ . The parameters are the same as in Fig. 1.

## B. The transition between fluid-sliding state and kink-dominated sliding state

When  $a/2\pi$  approaches an integer value the velocity-force characteristic of the fluid-sliding state develops a

relatively sharp transition step at a characteristic value of the applied force  $F$ . An example for  $a/2\pi = 1/20$  is shown in figure 7. For long enough chains no hysteresis is observable. For small chains we get bistability between different types of sliding states. Similar results has been found in a generalized FK model by Braun *et al.* [10,14,18]. The aim of this section is to answer the following obvious questions: What is the nature of the different sliding states? Why does the bistability depends on  $N$ ? Can we understand this transition and where does it occur?

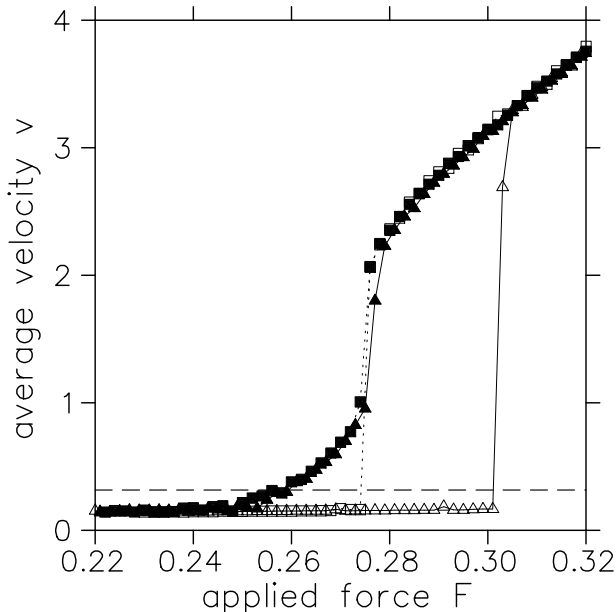


FIG. 7. The transition between the fluid-sliding state and the kink-dominated sliding state. The velocity-force characteristics for  $N = 500$  (filled symbols) and  $N = 200$  (open symbols) are shown. Squares and dotted lines (triangles and solid lines) indicate decreasing (increasing) applied force  $F$ . The rate  $|\dot{F}|$  is always  $10^{-7}$  except for  $N = 500$  and  $F \in (0.26, 0.29)$  where it is  $10^{-8}$ . The dashed line indicates the sound velocity which is equal to  $a$ . The parameters are  $a = \pi/10$ ,  $b = 2$ , and  $\gamma = 0.05$ .

First we take a more detailed look at the dynamics below and above the transition (see Fig. 8). The motion far below the threshold is almost regular. It corresponds to one of the multi-domain states we have discussed in the previous paper. There are two domain types, a stationary one with  $a = 0$  [it is responsible for the tilted lines in Fig. 8(a)] and a sliding one. Often the sliding domains are so small that they are actually  $2\pi$ -kinks, and larger sliding domains can be interpreted as clusters of  $2\pi$ -kinks [10]. That is, multi-domain states like the example of Fig. 8(a) are nonuniform distributions of  $2\pi$ -kinks. Thus, we call this state the *kink-dominated sliding state*. Note, that there are  $M$  kinks but no antikink.

It is well-known that kinks (and antikinks) cannot travel faster than the sound velocity (which is equal to one in our case). Each kink or antikink needs therefore at least  $N$  time units to travel through the whole chain. After that time a chain with  $M$  kinks will be shifted by  $2\pi M$ . Therefore, the average sliding velocity of a state like the one of Fig. 8(a) has to be less than  $2\pi M/N = a$ .

Fig. 7 shows that it is actually much below the sound velocity.

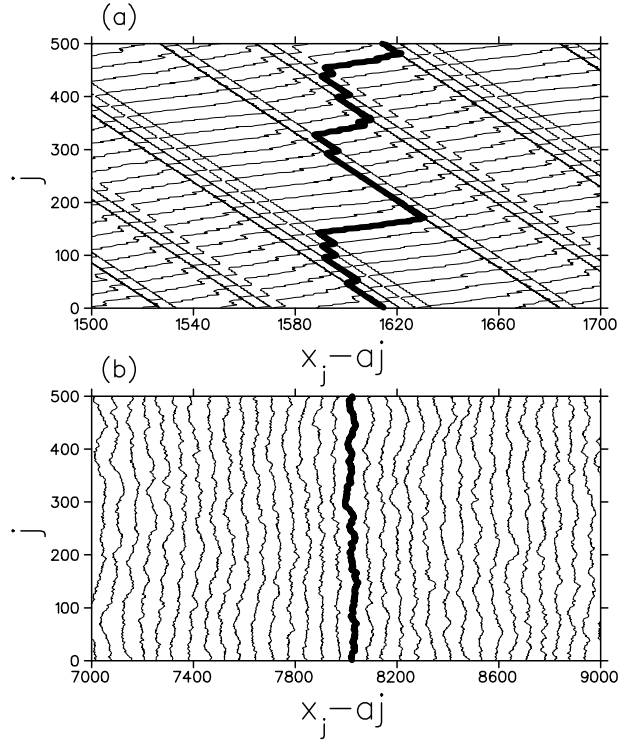


FIG. 8. The dynamics of the kink-dominated sliding state (a) and the fluid-sliding state (b). Several snapshots are shown taken at equidistant time steps (a)  $\delta t = 2\pi/v$  and (b)  $\delta t = 20\pi/v$ . In each case a particular snapshot is highlighted. The parameters are (a)  $F = 0.2$  and (b)  $F = 0.3$  and  $N = 500$ ,  $M = 25$ , (i.e.,  $a = \pi/10$ ),  $b = 2$ , and  $\gamma = 0.05$ .

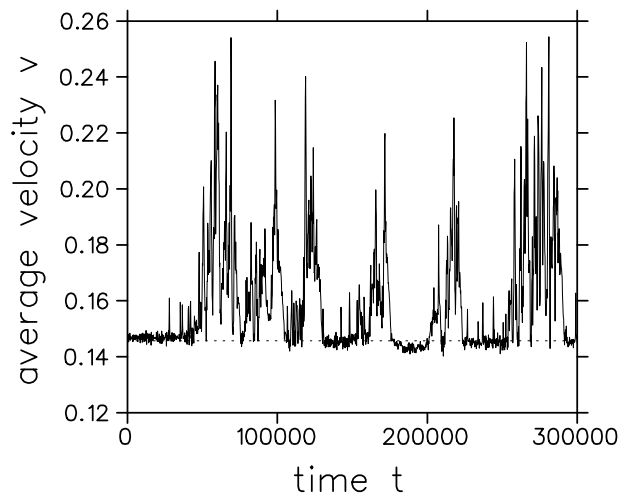


FIG. 9. The average sliding velocity  $v$  (averaged over intervals of 200 time units) as function of time. The velocity  $v_0$  of the quiescent phase is denoted by a dotted line. The parameters are  $N = 500$ ,  $M = 25$ , (i.e.,  $a = \pi/10$ ),  $b = 2$ ,  $\gamma = 0.05$ , and  $F = 0.24$ .

If the transition point is approached from below, the behavior depends on whether the chain is long or short. For long chains with many kinks, the average sliding velocity  $v$  starts to increase with  $F$  faster and faster. Later

on the increase slows down. We define the transition point  $F_{\text{FKT}}$  as the value of  $F$  where the slope of  $v(F)$  has a maximum. After the transition point the system is in a fluid-sliding state [see Fig. 8(b)]. All kinks (and antikinks) have disappeared, and the system is completely spatio-temporally chaotic. A short chain with only a few kinks still stays in the kink-dominated regime beyond  $F_{\text{FKT}}$ . Eventually, it jumps to the fluid-sliding state or to the solid-sliding state (see Fig. 7). A hysteresis occurs, and the chain goes back to the kink-dominated state at  $F \approx F_{\text{FKT}}$ .

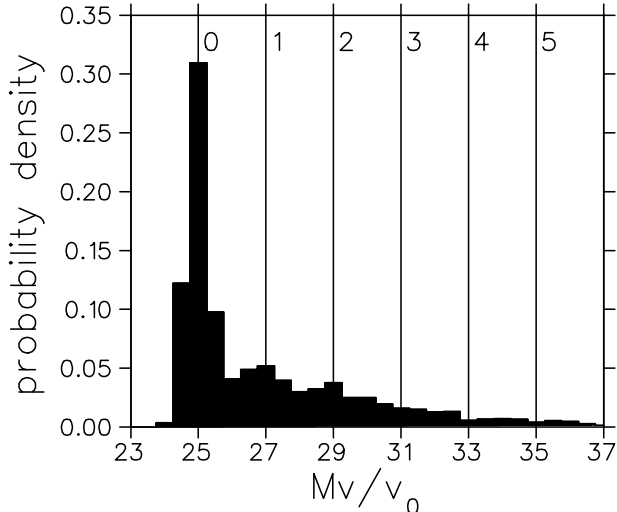


FIG. 10. The velocity distribution in the kink-dominated regime near the transition point. The statistics is obtained from 5000 samples. Each sample is the sliding velocity  $v$  averaged over 200 time units. The velocity of the quiescent phase is given by  $v_0 \approx 0.1457$ . The numbered vertical lines denote the number  $N_p$  of kink-antikink pairs. The parameters are the same as in Fig. 9.

At the transition point the sliding velocity strongly fluctuates. These fluctuations set in already much below the transition point. They lead to a larger value of the average sliding velocity compared to the value for small chains. A typical example is shown in figure 9. One sees bursts of activity above a level given by the value of  $v$  for small chains (see Fig. 7). A detailed look onto the dynamics of the chain reveals that an increase of  $v$  is caused by the *production of kink-antikink pairs* [10,14,18]. These pairs usually appear behind a  $2\pi$ -kink cluster. This may be the reason why for small chains the kink-dominated states survive beyond the transition point because the probability for a  $2\pi$ -kink cluster is too small. Each kink and antikink contributes to the sliding velocity of the chain. That is,  $v$  is given by

$$v = 2\pi \frac{M + 2N_p}{N} c_k, \quad (10)$$

where  $c_k$  is the velocity of the kinks and antikinks and  $N_p$  is the number of kink-antikink pairs. In the quiescent state without kink-antikink pairs, the average sliding velocity is given by  $v_0 = 2\pi M c_k / N$ . Thus the ratio  $v/(v_0/M)$  gives directly the total number of kinks and antikinks (i.e.,  $M + 2N_p$ ). Figure 10 depicts the distribution of the sliding velocity shown in Fig. 9. In addition

to the large peak at the quiescent state one sees clearly small peaks for  $N_p = 1$  and 2.

For  $a$  approaching zero (or any other integer multiple of  $2\pi$ ) the average sliding velocity of the kink-dominated sliding state also approaches zero. It disappears at  $a = 0$ . Thus, the system goes from the fluid-sliding state directly to a stationary state when  $F$  is decreased below the transition point  $F_{\text{FKT}}$ . If the value of  $b$  is not too large [i.e.,  $b = \mathcal{O}(1)$ ], the stationary state will be the ground state [19]. The transition is often accompanied by transients where a few kink-antikink pairs survive for a considerably long time. But in all simulations these pairs eventually disappeared.

We found that the transition point  $F_{\text{FKT}}$  is nearly independent of  $a$  (as long as  $a/2\pi$  is near an integer value). Table I shows that  $F_{\text{FKT}}$  increases with  $b$  weaker than linearly.

In order to understand the transition between the fluid-sliding state and the kink-dominated sliding state we compare the FK model with a simpler model, namely, one particle in a tilted spatially periodic potential plus additive white noise. This model was studied in details by Risken and Vollmer [5,20]. The single particle and the noise correspond to the center of mass of the FK model and the chaotic motion of the internal degrees of freedom, respectively. Of course the noise is neither additive nor white. Its strength depends on the state. It is obvious that the solid-sliding state and the stationary state of the FK model correspond to the running state and the locked state of the simple model in the absence of noise. We suggest that the fluid-sliding state and the kink-dominated state of the FK model correspond also to the running and locked states of the simple model but now with noise. Risken and Vollmer showed that the bistability between the running state and the locked state disappears even for infinitesimally weak noise. There is a well-defined transition point  $F_2$  which is smeared out for increasing noise strength. For  $\gamma \ll \sqrt{b}$  it is given by

$$F_2 = 3.3576\gamma\sqrt{b}. \quad (11)$$

Thus we expect  $F_{\text{FKT}} \approx F_2$ . Table I shows that this is indeed the case especially for small values of  $b$ .

TABLE I. The transition point  $F_{\text{FKT}}$  between fluid-sliding states and kink-dominated sliding states and the transition point  $F_2$  between the running state and the locked state of single particle in a periodic potential under the influence of weak noise. The parameters are  $N = 500$ ,  $M = 0$ , and  $\gamma = 0.05$ .

$b$	$F_{\text{FKT}}$	$F_2$
0.25	0.096	0.0840
0.5	0.130	0.1187
1	0.187	0.1679
2	0.276	0.2374
3	0.362	0.2908
4	0.444	0.3358
5	0.519	0.3754

### III. NONEQUILIBRIUM FREEZING AND MELTING

The aim of this section is to take a closer look at the hysteresis loop between stationary states and the fluid-sliding state (see Fig. 1). There are two different types of transitions. A depinning-pinning transition where the (chaotically) sliding chain turns into a stationary one. It is a kind of nonequilibrium freezing and, as in usual first-order phase transitions, the chain can be “supercooled” below the transition point  $F_{DP}$ . That is, for  $F$  slightly below  $F_{DP}$  the chain does not freeze immediately. It takes a while until a critical nucleus has appeared. The second transition is the pinning-depinning transition. The transition point  $F_{PD}$  depends on the stationary state and therefore on the history of the system. In an actual experiment where one sweeps through the hysteresis loop at a finite rate, one will therefore not get well-defined transitions points but more or less broad distributions. An example of such a (numerical) experiment is shown in the inset of Fig. 1(a). It is typical that the distribution of  $F_{DP}$  is narrower than the distribution of  $F_{PD}$ . For a quasistatic sweep the distribution of  $F_{DP}$  becomes sharp, whereas the width of the distribution of  $F_{PD}$  is nearly independent on the sweeping rate.

From equilibrium thermodynamics it is well-known that melting and freezing occur at the same temperature and the transition is of first-order. In our case far from thermal equilibrium the situation is different. In the overdamped limit the pinning-depinning transition point  $F_{PD}$  is identical with the depinning-pinning transition  $F_{DP}$  but the transition is of second order [21,22]. In the underdamped case we have bistability between sliding states and stationary states, i.e.,  $F_{DP} < F_{PD}$ .

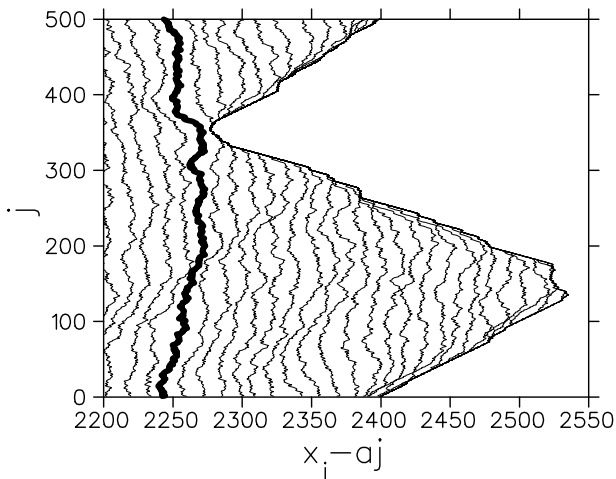


FIG. 11. Nucleation of a stationary state in the depinning-pinning transitions. The time step between two snapshots is  $\delta t = 4\pi/v$ . The snapshot just before nucleation is highlighted. The parameters are  $N = 500$ ,  $M = 160$ ,  $b = 2$ ,  $\gamma = 0.05$ , and  $F = 0.097$ .

A further characteristic feature of nonequilibrium melting and freezing is the change of the effective temperature [see e.g. Fig. 1(b)]. This is a general property which is also found in similar models with nonzero temperature of the environment [10,12,13]. That is, the

fluid-sliding state has an effective temperature which is *independent* on the temperature of the environment as long as the latter one is considerably less than the former one. The effective temperature is a measure of the enhanced energy flow due to the excitation of phonons.

#### A. Freezing: The depinning-pinning transition

We have studied in detail the depinning-pinning transition from a fluid-sliding state to a stationary state. We have chosen a value of  $a$  where the fluid-sliding state is completely spatio-temporally chaotic. Like in an ordinary first-order phase transition at thermal equilibrium the transition is caused by a *nucleation process*. That is, a small portion of the chain becomes stationary, and the fronts between this stationary nucleus and the sliding chain propagate into the chain. An example of such a nucleation process is shown in figure 11. One sees that states appear behind the fronts which can be characterized by an average particle distance  $a$  (or density  $1/a$ ) which is roughly constant. Note that the values of  $a$  behind both fronts have to be different. This can be understood by the following argument. In the previous paper we have seen that because of the conservation of the number of particles the velocity of a front traveling from one particle to the next is given by  $c = (v_1 - v_2)/(a_2 - a_1)$ , where the average particle distance and the average sliding velocity on both sides of the front are given by  $a_{1/2}$  and  $v_{1/2}$ , respectively. The chaotic sliding state is characterized by  $a_1 = 2\pi M/N$  and  $v_1 > 0$ . For the stationary state  $v_2 = 0$  holds. In order to have fronts traveling in opposite directions (see Fig. 11) the average particle distances of the stationary states have to be different (one larger than  $a$  and one smaller than  $a$ ). We found that they are always the nearest integer multiples of  $\pi$ , that is, for  $0 < a < \pi$  they are zero and  $\pi$ . From this consideration it is clear that after the depinning-pinning transition the system cannot be in the ground state [19] which is characterized by a single domain with a uniform  $a$ . Instead the chain will be in a stationary *two-domain state* which is not quite perfect because each domain contains defects at low density.

A similar depinning-pinning transition was found in a seemingly completely different model, namely, the quenched Kadar-Parisi-Zhang equation with negative nonlinearity [23]. It is a nonlinear diffusion equation which models the surface growth in disordered media. Here the dissipation is strong and the randomness of the pinning landscape is important contrary to the weakly damped FK model. Nevertheless the pinning-depinning transition is of first order and the state which freezes out of the sliding state is a two-domain state, as in the FK model (compare Fig. 2 of Ref. [23] with Fig. 11).

The duration of freezing  $t_D$  is the sum of the nucleation time  $t_N$  and the growth time  $t_G$ . The nucleation time is the time that evolves until a critical nucleus appears. A critical nucleus is a nucleus which is large enough to grow into the fluid-sliding state. The nucleation time  $t_N$  will be a Poisson distribution if the probability for the appearance of a critical nucleus in a short time-step is

small, i.e.,

$$\rho(t_N) = \theta^{-1} e^{-t_N/\theta}. \quad (12)$$

It is well-known that the average and the standard deviation of a Poisson-distributed value are identical, i.e.,  $\langle t_N \rangle = \Delta t_N = \theta$ . For systems much larger than the critical nucleus, the probability for nucleation increases linearly with the system size, i.e.,  $\theta \sim 1/N$ .

The time  $t_G$  for a critical nucleus to grow up to the stationary state does not fluctuate as strongly as  $t_N$  because it is roughly given by the system size divided by the sum of front velocities. Thus  $\langle t_G \rangle \sim N$ .

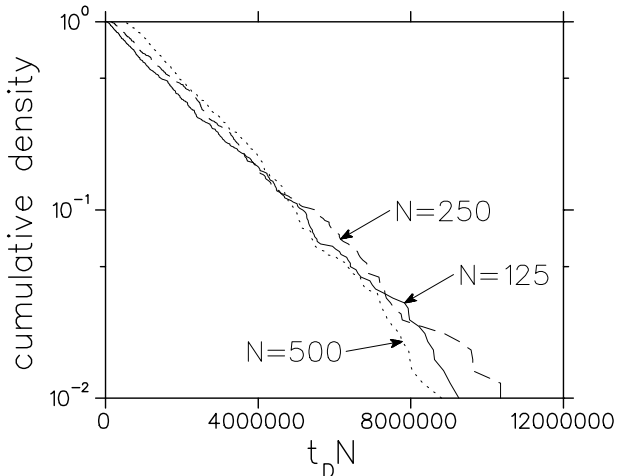


FIG. 12. Cumulative density of the duration times  $t_D$ . Each curve is obtained from 500 numerical nucleation experiments. The parameters are  $a = 16\pi/25$ ,  $b = 2$ ,  $\gamma = 0.05$ , and  $F = 0.097$ .

Figure 12 shows that the nucleation process is indeed characterized by a Poisson distribution with  $\theta \sim 1/N$ . From fits of the curves shown in Fig. 12 we found  $\theta N = (2.1 \pm 0.1) \cdot 10^6$ . One can also see a shift of the distribution for increasing  $N$  to larger values of  $t_D$ . This reflects the fact that  $\langle t_G \rangle$  increases with  $N$ .

For values of  $a$  between 2.45 and 3.09 (and  $b = 2$ ,  $\gamma = 0.05$ ,  $N = 500$ , and  $F \approx F_{\text{FKT}}$ ) we found that the fluid-sliding state changes its character. A domain appears where the particles are stationary (with two particles per potential well). This domain which is surrounded by spatio-temporal chaos has a constant size and travels through the chain with a constant velocity. The transition from this so-called *traffic-jam state* [10] to a stationary one occurs also via nucleation. The critical nucleus seems to appear always at the back of the stationary domain. It reverses the propagation direction of the front. That is, the chaotic state stops traveling into the stationary one. Instead a front propagates into the chaotic state leaving behind a stationary state different from the already existing one. Thus the result is again a stationary two-domain state where one domain already exists at least partially before the transition. The nucleation probability is roughly independent of the system size  $N$  because the nucleation site is predetermined.

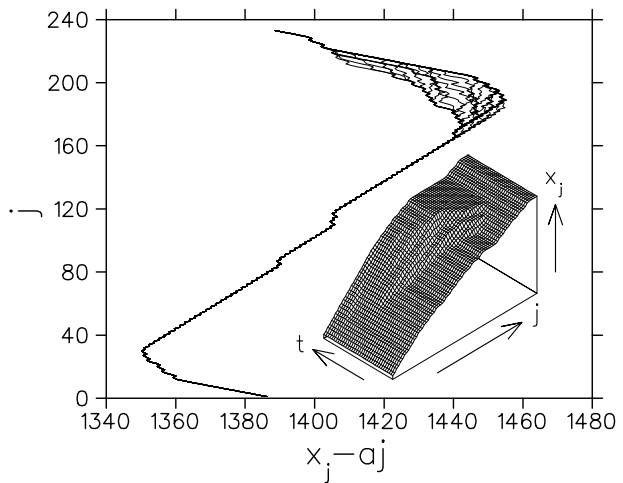


FIG. 13. An example of a micro-slip. Snapshots at an interval of 10 time units are shown. The inset shows  $x_j$  for  $j \in [160, 233]$ . The parameters are  $N = 233$ ,  $M = 89$ ,  $b = 2$ ,  $\gamma = 0.05$ , and  $F$  from 0.11554 until 0.115575 at a rate of  $10^{-7}$ .

## B. Melting: Pinning-depinning transition

The transition from a stationary chain to a sliding one is the pinning-depinning transition. The transition point  $F_{\text{PD}}$  depends on the stationary state. It corresponds to a saddle-node bifurcation where the particular stationary state annihilates with an unstable stationary state. In the overdamped limit  $F_{\text{PD}}$  is uniquely defined by the saddle-node bifurcation of the last stable stationary state which is usually the state which develops adiabatically out of the ground state for  $F = 0$ . The disappearances of the other stationary states in a saddle-node bifurcation lead only to more or less local rearrangements of the chain. We call such a rearrangements a *micro-slip*. A micro-slip changes the center of mass of the chain but does not lead to sliding. An example is shown in figure 13. This behavior and the statistics of micro-slips has been studied mainly in models with random external potential [24,25].

In the underdamped regime the energy gained from a local rearrangement is not dissipated immediately. This may lead to an avalanche which turns the whole system into a sliding state. Whether a saddle-node bifurcation leads to a micro-slip or to a transition to sliding depends on the stationary state and on the damping constant  $\gamma$ . For each stationary state one can presumably find a critical value  $\gamma_c$  which distinguishes both cases: For  $\gamma > \gamma_c$  we get a micro-slip, otherwise a transition to sliding. In our simulations we found only a few (not more than three) micro-slips for  $\gamma = 0.05$  and  $b = 2$ . The pinning-depinning transition point depends strongly on the history of the system because the actual value of  $F_{\text{PD}}$  depends on the stationary state. Sweeping several times through the pinning-depinning hysteresis loops, we find a broad distribution of  $F_{\text{PD}}$  even for very small sweep rates.



#### IV. SUMMARY AND CONCLUDING REMARKS

In this paper we have shown that in the *weakly* damped and strongly driven FK model spatio-temporal chaos appears. This chaotic state, called *fluid-sliding state*, has an effective temperature which reflects the fact that phonons are excited. This has to be contrasted by the solid-sliding state where no phonons are excited [26]. The excitation of phonons opens up additional channels of dissipation. Thus friction in the fluid-sliding state is larger than in the solid-sliding state.

The velocity-force characteristic shows a pronounced transition if the average particle distance  $a$  is near but not identical to an integer multiple of the period of the external potential. It is a transition between the kink-dominated sliding state and the fluid-sliding state. Below the transition point  $F_{\text{FKT}}$  sliding is caused by the propagation of  $2\pi$  kinks. Approaching the transition point from below leads to an increasing production of kink-antikink pairs. Above the transition point all kinks and antikinks disappear and the chain is in the fluid-sliding state with an average sliding velocity which depends only weakly on the average particle density  $1/a$ . In the kink-dominated regime the average sliding velocity is proportional to  $a \bmod 2\pi$ . The transition point  $F_{\text{FKT}}$  is roughly independent of  $a$ . For small values of  $b$  it is very well approximated by the transition point between the running and locked solution of an ( $N = 1$ )-FK model with infinitesimally small additive white noise [i.e. Eq. (11)]. This raises the question whether the dynamics can be reduced to a center-of-mass motion plus some nontrivial (e.g. colored, state-dependent) noise term.

The nonequilibrium freezing (i.e., the transition from sliding to stationarity) of the fluid-sliding state is a nucleation process. The resulting stationary state has two domains of different particle densities.

The nonequilibrium melting (i.e., the transition from a stationary state to sliding) of such a stationary state corresponds to a saddle-node bifurcation where the stationary and, of course, the stable state annihilates with its unstable counterpart. In the case of nonzero environmental temperature the transition occurs a bit earlier because thermal activation overcomes the barrier which decreases to zero at the saddle-node bifurcation. Not all saddle-node bifurcations lead to melting. They may lead to a local rearrangement of the particle configuration called micro-slip. The pinning-depinning transition point depends on the history because each stationary state has another bifurcation point.

Our results are qualitatively very similar to results of similar models. Persson studied a two-dimensional Lennard-Jones liquid on a corrugated potential with square symmetry at a nonzero temperature [12]. He varied the temperature between  $1/3$  and  $1/2$  of the melting temperature (the thermal energy was roughly a tenth of activation energy for single particle diffusion). He obtained velocity-force characteristics and effective temperature plots similar to Fig 1. Because of the relatively high temperature of the environment he did not find hysteresis between the solid-sliding state and the fluid-sliding state. As in the FK model, the transition from the fluid-

sliding state to a stationary state is also a nucleation process. Persson found that it occurs when the effective temperature is equal to the melting temperature at thermal equilibrium. Because the velocity distribution of the fluid-sliding state was Gaussian, he argued that the fluid-sliding state is in a kind of thermal equilibrium. Therefore it has to freeze below the melting temperature. But as we have seen in Sec. II A, Gaussian distributed velocities do not imply a quasi-thermal equilibrium. It would be interesting to look whether in Persson's model the equipartition theorem of the phonon modes is fulfilled or not. This is clearly a better test on thermal equilibrium.

Granato *et al.* studied a two-dimensional Frenkel-Kontorova model at nonzero temperatures [13]. The external potential is corrugated only in the direction of the applied force. Also the particles can move only in this direction. They did the simulations at a temperature which corresponds to  $1/4$  of the activation energy and which is roughly  $1/5$  of the melting temperature. They also found a behavior like in Fig. 1 again without a hysteresis between the solid-sliding state and fluid-sliding state. They also confirmed the observation of Persson that the transition from sliding to stationarity occurs at the melting temperature.

Braun *et al.* investigated a generalized FK model that is quite similar to the model studied by Persson [10,14,18]. The main difference is that the substrate potential is anharmonic and the interaction potential is an exponential repulsion. They did the simulations mainly for two different temperatures which correspond to  $10^{-3}$  and  $1/20$  of the activation energy for single particle diffusion. They report results for one-dimensional chains of atoms as well as for two-dimensional layers. There seems to be no qualitative differences between one and two dimension. Again velocity-force characteristics and effective temperature plots are similar to our results. They found a hysteresis between solid sliding and fluid sliding. Its width decreases with the environmental temperature and disappears eventually (at a temperature which is roughly  $1/5$  of the activation barrier for hopping of uncoupled single particles). Near fully commensurate particle densities they found a transition (denoted by  $F_{\text{pair}}$ ) which is similar to the transition from the kink-dominated sliding regime to the fluid-sliding regime of the FK model. Because their chain was short (i.e.,  $N = 105$ ) this transition shows hysteresis for very low temperatures. Instead of a fully chaotic fluid-sliding regime they always found two-domain states with alternatively running and locked particles (traffic-jam regime). They also measured the transition point  $F_{\text{pair}}$  as function of the damping constant [18]. It increases roughly linear with the damping constant but the authors seemed not to be aware that (11) is again a remarkable good approximation (i.e. errors are less than 10%) for  $F_{\text{pair}}$ .

#### ACKNOWLEDGMENTS

We thank H. Thomas for critical reading of the manuscript. We also acknowledge the possibility to do simulations on the NEC SX-3 and SX-4 at the Centro

Svizzero di Calcolo Scientifico at Manno, Switzerland.  
This work was supported by the Swiss National Science  
Foundation.

---

- [1] M.A. Rubio, C.A. Edwards, A. Dougherty, and J.P. Golub, *Phys. Rev. Lett.* **63**, 1635 (1989).
- [2] S. He, G. Kahamanda, and P.-Z. Wong, *Phys. Rev. Lett.* **69**, 3731 (1992).
- [3] G. Blatter, M.V. Feigel'man, V.B. Geshkenbein, A.I. Larkin, and V.M. Vinokur, *Rev. Mod. Phys.* **66**, 1125 (1994).
- [4] G. Grüner, *Rev. Mod. Phys.* **60**, 1129 (1988).
- [5] H. Risken, *The Fokker-Planck Equation*, (Springer, Berlin, 1984).
- [6] T. Natterman, S. Stepanow, L.H. Tang, and H. Leschom, *J. Phys. II (France)* **2**, 1483 (1992).
- [7] O. Narayan and D. Fisher, *Phys. Rev. B* **48**, 7030 (1993).
- [8] T. Kontorova and J. Frenkel, *Z. Phys. Sowjetunion* **13**, 1 (1938).
- [9] S. Watanabe, H.S.J. van der Zant, S.H. Strogatz, and T.P. Orlando, *Physica D* **97**, 429 (1996).
- [10] O.M. Braun, T. Dauxois, M.V. Paliy, and M. Peyrard, *Phys. Rev. Lett.* **78**, 1295 (1997); *Phys. Rev. E* **55**, 3598 (1997).
- [11] T. Strunz and F.J. Elmer, previous paper.
- [12] B.N.J. Persson, *Phys. Rev. B* **48**, 18140 (1993).
- [13] E. Granato, M. R. Balcan, and S. C. Ying, in *The physics of sliding friction*, B. N. J. Persson and E. Tosatti (eds.), (Kluwer Academic Publishers, Dordrecht, 1996).
- [14] O.M. Braun, A.R. Bishop, and J. Röder, *Phys. Rev. Lett.* **79**, 3692 (1997).
- [15] M.C. Cross and P.C. Hohenberg, *Rev. Mod. Phys.* **65**, 851 (1993).
- [16] J.P. Eckmann and D. Ruelle, *Rev. Mod. Phys.* **57**, 617 (1985).
- [17] By the way, we checked in microcanonical simulations of the thermal equilibrium (i.e., no damping,  $\gamma = 0$ , no driving,  $F = 0$ ), that for the same values of  $b$  and  $T$  as in Fig. 6 the kinetic energy  $e_k$  of the phonon modes are indeed equipartitioned.
- [18] M. Paliy, O. Braun, T. Dauxois, and B. Hu, *Phys. Rev. E* **56**, 4025 (1997).
- [19] More precisely: The state which develops adiabatically out of the ground state of the undriven system (i.e.,  $F = 0$ ).
- [20] H.D. Vollmer and H. Risken, *Z. Phys. B* **37**, 343 (1980).
- [21] S.N. Coppersmith and D.S. Fisher, *Phys. Rev. A* **38**, 6338 (1988).
- [22] L.M. Floría and J.J. Mazo, *Adv. Phys.* **45**, 505 (1996).
- [23] H. Jeong, B. Kahng, and D. Kim, *Phys. Rev. Lett.* **77**, 5094 (1996).
- [24] A.A. Middleton and D.S. Fisher, *Phys. Rev. Lett.* **66**, 92 (1991).
- [25] O. Pla and F. Nori, *Phys. Rev. Lett.* **67**, 919 (1991).
- [26] There is one exception, namely, the phonon with the same wave number as the washboard wave. But its amplitude is very small (see Sec. III.B in Ref. [11]).